Climate Dynamics (2003) 21: 77–89
DOI 10.1007/s00382-003-0319-3

W. Qian · Q. Hu · Y. Zhu · D.-K. Lee

Centennial-scale dry-wet variations in East Asia

Received: 29 August 2002 / Accepted: 20 January 2003 / Published online: 14 May 2003

Abstract This study attempts to combine four independent long-term climatic data and modern observations into one cohesive set; to describe the spatial and temporal patterns of variability of dry and wet periods in East Asia over the past one thousand years; and to examine physical causes of the pattern variations. The data include the 220-year observed precipitation in Seoul, South Korea, the dryness-wetness intensity data in eastern China for the last 530 years, and other two independent chronologies of dryness-wetness grades in the past millennium in eastern China based on instrumental observations and historical documents. Various analysis methods including wavelet transform and rotated empirical orthogonal function were used in revealing climate variations from these datasets. Major results show that the dry and wet anomalies initially appeared in the north part of eastern China and then migrated southward to affect south China. This process is repeated about every 70 years. However, in contrast in the last two decades of the twentieth century a dry situation appeared in north China and a wet climate predominated in the south part of the country. The multidecadal variations of the monsoon circulation in East Asia and the thermal contrast between inland Asia and its surrounding oceans may contribute to the dry-wet phase alternation or the migration of dry-wet anomalies. In regional scale variations, a consistent dry or wet pattern was observed spreading from the lower Yangtze River valley to South Korea. Frequencies of severe dry-wet situations were low in the eighteenth and nineteenth century and they were higher in the twentieth century. The recent increasing trend in frequencies of severe dry-wet chances occurred along with global warming and regional climatic changes in China.

W. Qian (✉) · Y. Zhu
Monsoon Environment Research Group,
Department of Atmospheric Sciences,
Peking University, Beijing 100871, China
E-mail: qianwh@pku.edu.cn

Q. Hu
Climate Bio-Atmospheric Sciences Group,
School of Natural Resource Sciences,
University of Nebraska-Lincoln, Lincoln,
NE 68583-0728 USA

D.-K. Lee
Atmospheric Sciences,
School of Earth and Environmental Sciences,
Seoul National University, Seoul 151, South Korea

1 Introduction

In China, droughts and floods have caused the largest economic losses among all natural disasters in 1949–1995 (Damage Report 1995). During these 47 years, there were 12 severe droughts occurring in at least one of the major river basins in China. These droughts seemed clustered in three periods i.e. 1959–1961, 1978–1982 and 1986–1994. In 1986–1994, for example, six severe droughts occurred. In the last decade alone, three major floods also occurred in the summers of 1991, 1998, and 1999 in the lower Yangtze River valley and northeastern China, resulting in tremendous losses in human life and property damages. The frequent recurrence of the floods and droughts in recent decades suggests a rise in the frequency of severe droughts/floods in eastern and southern China. It is important to understand such changes in severe droughts/floods in the historical context and identify possible mechanisms for these disastrous climate events. Such an understanding will give us the ability to predict droughts/floods in the future.

To gain such knowledge, we need to first understand how droughts/floods varied in the past. This information may disclose long-term trends and multidecadal and centennial scale climate variations influencing the occurrence of droughts/floods. Further understanding of the processes or causes of these trends and variations, may help us to identify the ones that can be used to project the course of future climate (Bradley and Jones 1992). In this study, we examine historical data for the

last 1000 years in the East Asia in order to understand centennial-scale alternations of the region's wet and dry climate and potential causes of the variations.

China, Korea, and Japan are located in East Asia. Previously, rainfall patterns of these three countries have been investigated separately, and little attention has been given to relationships of regional rainfall patterns (Qian et al. 2002). For example, the dry-wet variations can be found from individual studies for different historical periods for Korea (Cho and Na 1979; Kim 1992; Lim and Jung 1992), Japan (Murata 1992), and eastern China (Wang and Zhao 1979; Ronberg and Wang 1987; Wang 1988; Jiang et al. 1997; Song 1998, 2000; Hu and Feng 2001; Qian and Zhu 2001, 2002). As yet, no cohesive understanding has been developed. In order to understand long-term droughts/floods variations in East Asia a long-term series of wet-dry data needs to be developed from the different data sources.

To develop such a cohesive historical dataset, we use modern observations and several historical dry-wet data series derived from ancient Chinese documents. These historical data series were used in several previous studies, but only a single data series was applied in individual studies. In this study of droughts/floods variations, we construct a cohesive data series from the existing historical data series. These data series are described in the next section, followed by discussion in Sect. 3 on their extension to recent decades using the instrumentation records. In Sect. 4, we use the data and derive the dry-wet principle components and their variations from rotated empirical orthogonal function and wavelet transform calculations. In Sect. 5, previous approaches used to derive frequency of wetness/dryness are reviewed, and dry-wet intensity changes in six regions in China are derived from historical data series. In Sect. 6, indices measuring wetness and dryness in eastern China for the past 1000 years are obtained and their variation relationships in different river basins are analyzed. In Sect. 7, the derived data are used to examine centennial-scale variations in wetness and dryness and their relationship with variations in the East Asian monsoon systems. Multidecadal circulation change and its possible forcing effect on dry/wet anomalies are examined in Sect. 8. Section 9 contains the conclusions.

2 Data sources

2.1 Dry-wet intensity (DWI)

Since the 1970s, Chinese climatologists have collaborated in an effort to extract climatic information from over 2000 historical documentary records for the last 530 years beginning in 1470. These records included the government weather book "Clear and rain records" and local government drought/flood reports and private diaries. A product of this effort is the *Yearly charts of dryness/wetness in China for the last 500 years* (Central Meteorological Bureau 1981). In this dataset, the summer season climate (May–September) was categorized into dry and wet intensity (DWI) on a scale of 1 to 5, from very wet (flood, 1), wet (2), normal (3), dry (4), and very dry (drought, 5), for each summer in the 530 years from 1470 to 1999 for 120 sites in China. The DWI records in this dataset for the recent decades after instrumentation observations became available are calculated from measured rainfall in the months of May–September based on methods described in Tang (1988), Zhang'D (1988), and Zhang and Crowley (1989). Statistical properties, for example, consistency and persistency, of this DWI data series have been carefully examined and established (Yao 1982; Ronberg and Wang 1987).

Recently, this unique historical dataset has been used to understand climate variations in China. For instance, Hu and Feng (2001) analyzed the DWI data (1470–1997) from 65 of the 120 sites and found a centennial-scale southward migration of droughts/floods in eastern China. Song (2000) used data from 100 of the 120 sites (1470–1998) and studied changes in dryness/wetness in different centuries. Zhou et al. (2002) studied chaotic features of floods using data from the sites in the Huaihe River Basin over the time period 1470–1991.

In this study, we use the DWI data from 100 sites in eastern China from 1470 to 1999 (Fig. 1). This data length and spatial coverage are similar to that in Song (1998, hereafter S98) but our study subjects and analysis methods are different.

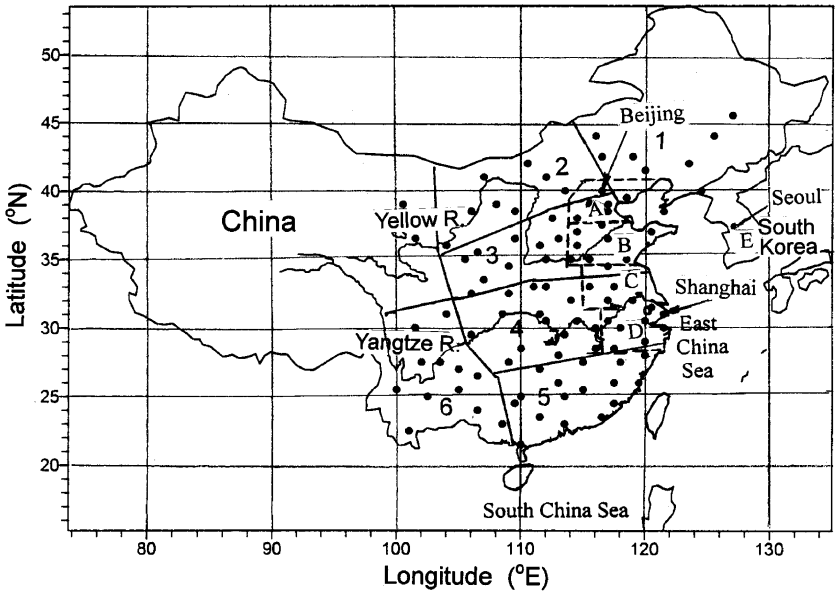

Fig. 1 Geographic distribution of the 100 sites selected in eastern China. Geographical location of the six study regions: *1* is northeast China, *2* is northern north China, *3* is the mid- and lower Yellow River, *4* is the mid- and lower Yangtze River, *5* is south China, and *6* is southwest China. The lettered regions, *A, B, C, D*, and indicate four regions divided by the *dashed lines* in east China and E is South Korea. The Yellow River and the Yangtze River are *labeled*

2.2 Wang's type (WT) and derived Wang indices (WI)

In a comparison analysis, Wang (1988) examined the empirical orthogonal function (EOF) derived from the data in *Yearly charts of dryness/wetness in China for the last 500 years*, and from instrumental data for the recent decades. His EOF results confirmed that the two data sets are nearly identical in spatial variations, confirming that the conversion from the instrumentation data to the wet/dry intensity scale is reliable. While examining the data consistency, Wang et al. (1987) explored additional historical sources of rainfall information and were able to extend the historical rainfall records from 1470 back to AD 950. With this data consistency, Wang (1988) extended his series to the last 1000 years, and found six wet-dry anomaly patterns in eastern China. He named them pattern A through F (Fig. 2) and used them to describe annual rainfall anomaly in eastern China from AD 950 to 1980. His result was a series of letters A to F for each year in the period. This chronology of rainfall anomaly patterns has been referred to as Wang's type (WT).

Although the WT series described variations of summer rainfall anomaly patterns, its letter series made it difficult for quantitative evaluation of multidecadal and centennial scale variations of wet-dry conditions in eastern China. To resolve this problem, we examined the six patterns and found that they can be paired in three groups, each of which has two patterns. In each pair, one pattern is a nearly reverse of the other as shown in Fig. 2. The top two panels in Fig. 2 are examples of a pair that has a wet summer in the eastern half of China, pattern A, and a nearly reversed pattern, pattern B, corresponding to a dry summer in the region. The middle pair in Fig. 2 has one pattern with wet summer in the mid and lower Yangtze River regions and dry conditions in both the north and south of the river basin, pattern C, has a reversed pattern, pattern D. Patterns E and F in the third pair in Fig. 2 have rainfall anomalies of opposite signs in northern and southern China with near average rainfall along the corridor of the Yangtze River.

These features in the WT allow us to define a scale to represent rainfall anomaly intensity in different regions in China. In particular, for the Yangtze River basin, pattern C with very wet conditions in the basin is assigned +2 and pattern D with very dry conditions in the area is assigned –2. In patterns A and B, the area has moderately wet and dry conditions and is assigned values +1 and –1, respectively. Because both patterns E and F correspond to nearly normal rainfall in the area, a 0 is assigned for the area. As a result, we have transformed the WT into a series of numerical indices describing intensity of summer rainfall anomalies. We named this index series Wang indices (WI). The WI for the Yellow River basin and southern China are defined in a similar manner and their scales and corresponding WT are given in Table 1.

2.3 Zhang's indices (ZI)

In addition to the WT, another series of indices describing dry-wet condition also were developed for a six regions in eastern China but only the four smaller coastal areas, A, B, C, and D have been used here (see Fig. 1). Region A covers the Hebei Province, including Beijing and Tianjing districts. Region B is in the lower part of the Yellow River and Shandong Province. Region C is in the Huaihe River Basin north of the lower Yangtze River. Region D is from

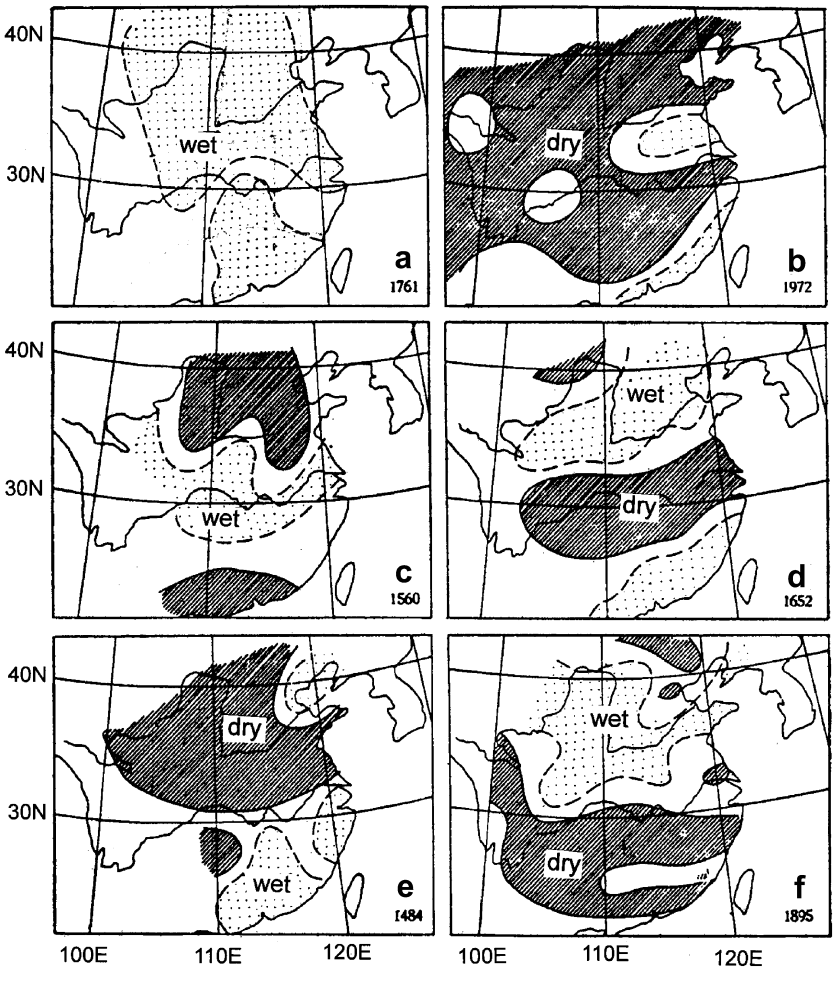

Fig. 2a–f Examples of the six different types in WT. The *shaded area* indicates dry and the *stippled area* denotes wet conditions in the specific years

south Jiangsu Province to Zhejiang Province south of the lower Yangtze River. Both the "Clear and rain record" of the eighteenth and the nineteenth centuries, which described primarily the dry-wet conditions in regions A and D, and additional documentary records discovered by Zhang and his colleagues, e.g. Jiang et al. (1997), describing the dry-wet conditions in Regions B and C were used to derive a 5-scale dry-wet intensity series for each of the four regions. These series have been referred to as Zhang's indices. In this study, we use Zhang's indices from 1777 to 1992 and analyze the dry-wet variations in the east coastal areas in China to compare them with variations in rainfall anomalies in Korea whose longest wet-dry records start from 1777 (see Sect. 2.5).

2.4 A comparison of the indices

To summarize the four dry-wet indices, i.e. DWI, WT, WI, and ZI, and their differences, we prepared Table 2. This shows that DWI has the largest spatial coverage and a total of 120 sites in China. It has a shorter time length from 1470 to 1999, however. The other three indices, particularly the ZI, are for relatively smaller regions but have a longer record length starting in AD 960. The indices, except for WT, have five similar numerical scales measuring intensity from very wet to very dry although WI uses a different numbering method. WI has three series for the Yellow River basin, Yangtze River basin, and south China from AD 950 to 1999. Indices ZI have four series for four regions along the east coasts of China from AD 960 to 1992.

The quality of the data series is similar because they were derived using similar data sources although ZI and WI (WT) may have used additional sources of historical documents from regional collections. Various evaluations of these indices for different historical periods have shown their consistency.

2.5 Korean rainfall (KR)

Korean rainfall (KR) data are used in our comparison of the rainfall variations with that in eastern China. The data are from instrumental records for the last century from a few sites in Korea. In addition, historical rainfall data in Seoul, Korea are used, and these data were produced from traditional Korean rain gauge measurements in Seoul from 1777 to the beginning of the last century (1907) (Lim and Jhun 1992; Jung et al. 2000). In the Korean rain gauge measurements, the precipitation amount was measured using Korean measurements such as "Pun", "Chi", and "Cha", which correspond approximately to 2, 20, and 200 mm, respectively. These early notations of rainfall were converted into modern numerical values with consistent accuracy (Cho and Na 1979; Lim and Jhun 1996).

Table 1 Characteristics and typical years of WT, and corresponding WI in the Yellow River valley, the Yangtze River valley, and south China

WT	Characteristics	Typical year	WI		
			Yellow River	Yangtze River	South China
(A)	Wet larger part	1761	+1	+1	+1
(B)	Dry all China	1972	–1	–1	–1
(C)	Wet in the Yangtze River	1560	0	+2	0
(D)	Dry in the Yangtze River	1652	0	–2	0
(E)	Wet south and dry north	1484	–2	0	+2
(F)	Wet north and dry south	1895	+2	0	–2

2.6 Atmospheric circulation data

It is perceived that dry-wet alternations in China, Korea, and Japan will be connected and affected by variations in various summer monsoon systems in East Asia. Several recent studies have shown that the seasonal shifts of the East Asia rainfall zones are linked to the movement of the monsoon fronts and the subtropical high in the northwest North Pacific (Lu 2001; Qian et al. 2002; Kim et al. 2002). Depending on the shift, the northward extension and intensity of the monsoon circulation in the summer months, moisture processes in the atmosphere and rainfall develop differently in eastern and northern China. Because the moisture advection is the largest near the 850 hPa level, moisture processes in the atmosphere associated with monsoon have often been evaluated using 850 hPa circulation. In this study, we examine summer season (June–August) atmospheric circulation changes and their relationship with the dry-wet conditions in China, using 850 hPa wind data and the 1000 hPa air temperature analyzed from the NCEP/NCAR Reanalysis Model (Kalnay et al. 1996; Kistler et al. 2001). The Reanalysis data have a spatial resolution of $2.5° \times 2.5°$ and are for the period 1948–2000. To reveal the anomalous features of summer rainfall in China for the recent times, meteorological data for the last 50 years from 160 stations in mainland China are used.

3 Analysis methods

Spectral analyses and wavelet transform methods are used in this study to reveal various variation components in the historical data series. Wavelet transform has been widely applied in signal detection from climate data series (e.g. Lau and Weng 1995; Jiang et al. 1997). The method is a powerful way to characterize the frequency, intensity, time position, and duration of variations in a climate data series. As a unique feature, the transform reveals localized time and frequency information without requiring the time series to be stationary as required by the Fourier transform and other spectral methods. Two kinds of function different in their symmetry are widely used in wavelet transform. A symmetric wavelet is the second derivative of a smoothing function and is optimal for finding maximum curvature in variations. The 'Mexican hat' wavelet is the second derivative of the Gaussian function, and is able to localize unstationary frequencies (Brunet and Collinean 1994).

We adopted the 'Mexican hat' wavelet in this study to analyze each dry-wet series and rainfall dataset. Details of the wavelet transform formulae and 'Mexican hat' functions are described in Jiang et al. (1997). According to the definition of the wavelet function, the scale parameter a represents the time-scale of the function. A smaller a value refers to a shorter scale or a higher frequency. The location parameter b corresponds to the time points in a year-to-year sequence. In order to detect climatic variations on decadal and centennial scales, we ran computations on the normalized time series (intensity indices) with the following time scale

Table 2 Similarities and differences of China dry-wet indices (DWI), Wang's type (WT), Wang indices (WI), and Zhang's indices (ZI)

Index name	DWI	WT	WI	ZI
Index value	5 classes	1 type/year	5 classes	5 classes
Data series	120	1	3	6
Spatial coverage	120 sites in China	Eastern China (3 river valleys)	Eastern China (3 river valleys)	6 regions in eastern China
Record length	1470–1999	950–1999	950–1999	960–1992

parameters: $a = 2, 3, \ldots, N/2$, through all data points, and $b = 1, 2, \ldots, N$ (N is the length of the series). Edge effects may occur originating at both the start and end point of a data series, magnifying or reducing values of the wavelet coefficients in an area near the end points, but the sign and other essential properties of the transform remain unchanged. The wavelet coefficients, $W(a, b)$, with positive or negative anomalies may represent the transitions between dry and wet condition on various time scales, a, and at different time points, b. $W(a, b) > 0$ corresponds to the dry condition while $W(a, b) < 0$ indicates a wet condition. A close pair of minimum and maximum centres of $W(a, b)$ may show an abrupt change from one persistent spell of anomaly to another anomaly of the opposite sign, leaving the required significance threshold as an open question (Brunet and Collinean 1994). If a frequency appears at a specific time scale, regular oscillation at the time scale exists.

Another method used in this study is the empirical orthogonal function (EOF) analysis. EOF provides a convenient method for studying the spatial and temporal variabilities. Because this method splits the spatial-temporal field into a set of orthogonal modes, it allows us to examine the spatial patterns and their temporal variations separately. If the modes are ordered, each successive mode explains the maximum amount of the remaining variance in the original field. Therefore, EOF is an effective method to compress the spatial-temporal field in both space and time. This feature, related to the data-adaptive nature of EOF, does not exist in other spectral analysis methods, such as Fourier analysis.

To seek physical modes with attractive properties, we also applied the rotated EOF (REOF) analysis (Richman 1981). REOF yields a new set of principle components (PCs, or modes) after we rotate the vector space of the initial EOFs to improve physical interpretations of the original field. Some details of the EOF have been reported in several studies (e.g. Richman 1981, 1986; Kelly and Jones 1999) and will not be repeated here.

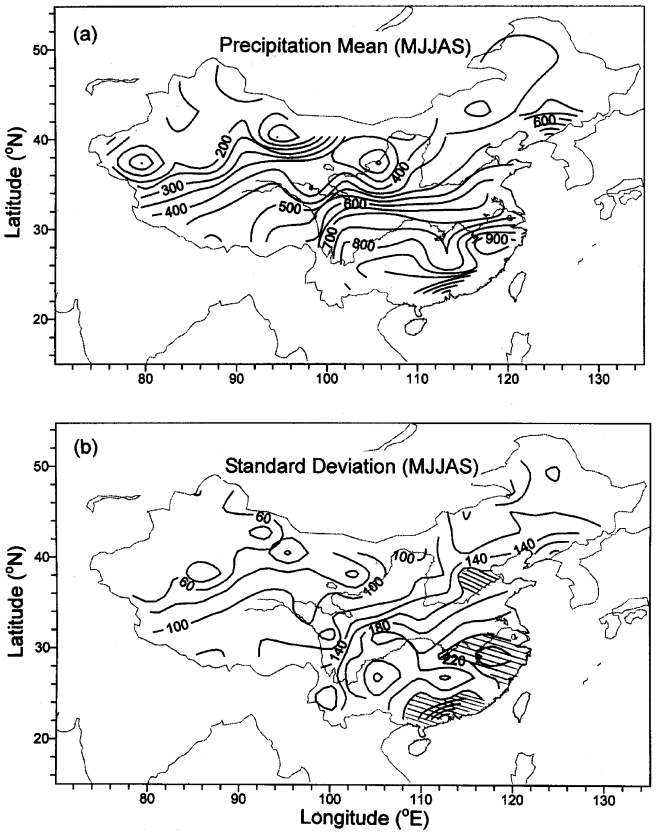

Fig. 3 **a** The averaged May–September total rainfall, and **b** May–September rainfall standard deviation from 1950 to 1999. Units are mm. In **B**, the *shaded areas* denote the relatively large standard deviations in the lower Yellow River, the lower Yangtze River, and south China

4 Dry-wet modes and their variations

We first examine the variations of the precipitation in China in recent decades. Figure 3 shows the total May–September precipitation averaged from 1950 to 1999 and its standard deviation based on 160-station data in China (Zhao et al. 1999). More precipitation is found in southern China and less in northern and western China. The standard deviation distribution reveals three large centres (hatched areas) in the lower Yellow River, the lower Yangtze River, and south China. In the rest of this study, we will focus on dry-wet alternations in these three centres.

REOF analysis on the 100-site DWI series for 530 years in China revealed six leading principal components (PCs) (Fig. 4). A five-year running mean was applied to the data series before the REOF calculation, in order to filter out high frequency variations. The first six PCs (or modes) explain a total of 64% (12%, 11%, 11%, 10%, 10%, and 10% for mode 1 to 6, respectively) of the variances of DWI. Six centres were found and marked by A, B, C, D, E, and F in the mid-reaches of the Yellow River and the Yangtze River, the lower-reaches of the Yellow River (similar to the eigenvector 2 of the EOF results in S98), the lower-reaches of the Yangtze River (similar to the eigenvector 3 in S98), south China, northern north China (similar to the eigenvector 4 in S98), and in the south central Yangtze River basin.

Interestingly, each of the six modes falls in one of the six divisions in Fig. 1, indicating different variation characteristics in each of the divisions. We pay special attention to those divisions along the east coast of China. Figure 5 shows the time series of the three modes centred in the lower Yellow River (division 3), the lower Yangtze River (division 4), and south China (division 5). The thick solid line for each mode indicates the 19-year running mean of the time series. In these time series, positive values denote dry conditions and negative values wet situations.

In our previous work (Qian and Zhu 2001), an analysis of annual precipitation for the last 120 years in seven sub-regions in eastern China showed that opposite signs of long-lasting or persistent precipitation anomalies were noted between north and south China with a secular variation starting from north China. Using the DWI series, Hu and Feng (2001) found a southward migration of centennial variations of dryness or wetness in the last 500 years in eastern China as well as in the western United States. Consistent with the migration result, the dashed-lines in Fig. 5, connecting the low points of the running curves, indicate similar migration of the wet maximum from one region to the next one south of it. A quasi-70-year oscillation can be inferred from the running curves. The last dashed-line indicates a

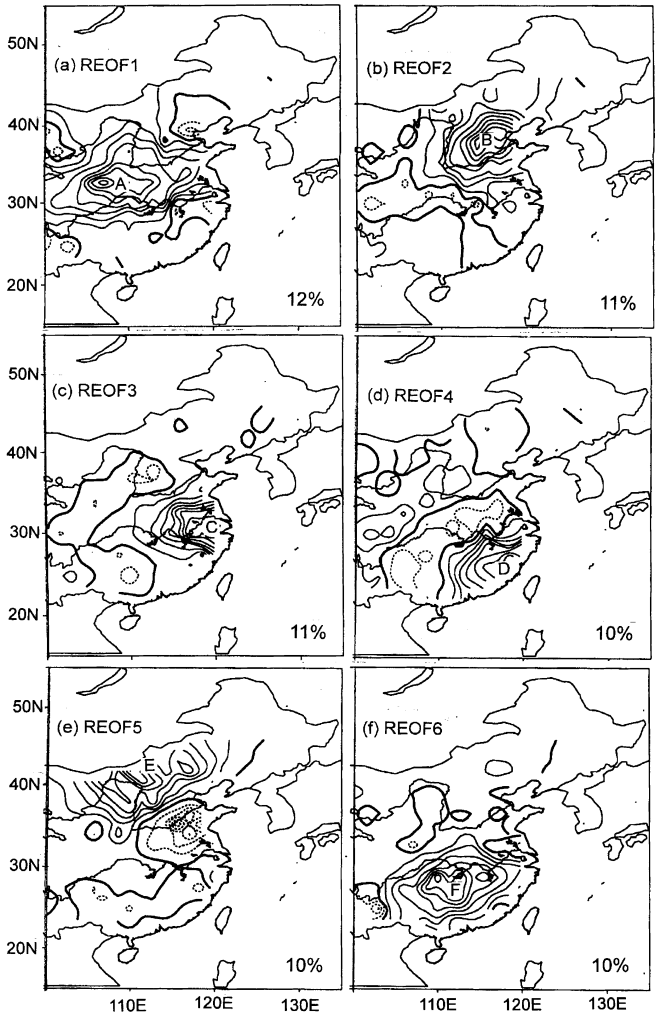

Fig. 4a–f The first six principal components of REOF for DWI in eastern China (see text for details). The interval is 0.1. The letters, *A, B, C, D, E*, and *F*, indicate the centres of modes. *Solid lines* denote positive REOF coefficients

similar southward migration with a wet maximum from the lower Yellow River in the early twentieth century, crossing the lower Yangtze River by 1940s, to south China in the 1950s and 1960s. It is interesting to notice that after the eighteenth century relatively regular oscillation and phase relations are found from these variations.

Zhu and Wang (2001) also showed an 80-year oscillation of summer rainfall in eastern China. By performing the wavelet transform from the third mode in the lower Yangtze River, a major dry-wet alternation at the time scale of about 70 years persisted since 1750s but an 80–90-year oscillation was noted in the earlier years (Qian and Zhu 2002). In the 70-year variation, two wet periods occurred in the last century, one in 1920s–1940s and another one stating since mid 1980s, a result consistent with the modern precipitation anomalies in China (Qian and Zhu 2001) and South Korea (Kim et al. 2002).

5 Severe dry-wet occurrences

In historical China, severe dryness or wetness anomalies spread in major river basins as discussed in the Introduction. Some studies investigated extreme events of short duration using high temporal resolution data (Yan and Yang 2001; Yan et al. 2002). Song (1998) studied the severe dry-wet occurrences at 100-year scale. Because quasi-20-year and quasi-70-year oscillations exist in China's rainfall records (Qian and Zhu 2001), an appropriate time scale for studying the extreme dry-wet conditions should be able to resolve the decadal scale. Accordingly, we use the decade as the time unit for extreme dry-wet occurrences and their frequency in the last five centuries. Because of the regional features depicted in Fig. 4, we examine the occurrence frequency of severe dryness and wetness in those individual regions. This occurrence frequency is represented by the percentage of severe dryness or wetness in each region, P^R, and calculated by

$$P^R = \left(\sum_{i,j}^{I,J} E_{i,j}^R \right) \Big/ (M \times Y) \ .$$

Here, M is the numbers of total sites in the region R, $Y = 10$ years and is the time interval between two data values, $E_{i,j}^R$ is the DWI that must equates to the grade 5 for severe dryness or grade 1 for severe wetness in region R for the i-th site in the region and j-th year, $I \leq M$, $J \leq 10$.

The frequencies of severe dryness and wetness are shown in Fig. 6. It shows no trend in severe dryness in northern north China. However, the variations in frequency show four epochs with higher ($>10\%$) than average and thus a higher frequency of severe dryness: 1480s–1540s, 1610s–1650s, 1720s–1760s, and 1870s. The recent period is longer than the previous three. A trend towards increasing frequency of severe wet conditions in northern north China can be seen in the last 530 years in Fig. 6b.

The frequency of severe dryness in the middle and lower Yellow River has two high periods, 1570s–1650s and 1910s-present, with a higher frequency in the former. There is no long-term trend of severe wetness in the middle and lower Yellow River but several features deserve attention. In the 1660s, the frequency of severe wetness reached 30% and in the 1900s it was over 20%. In the last century, relatively high frequency appeared before the 1920s and the 1960s–1970s while low occurrence frequency was found in the 1930s–1950s and 1980–1990s. These changes in the last century were consistent with the precipitation variations in northern China found in other studies (e.g. Qian and Zhu 2001).

In northeast China, similar variations in the frequency of severe dry-wet conditions are shown in Fig. 6 by the high percentages (20%) in the sixteenth century and the twentieth century and a low percentage (less than 10%) in the eighteenth century. The frequency of severe dryness increased rather significantly since the last

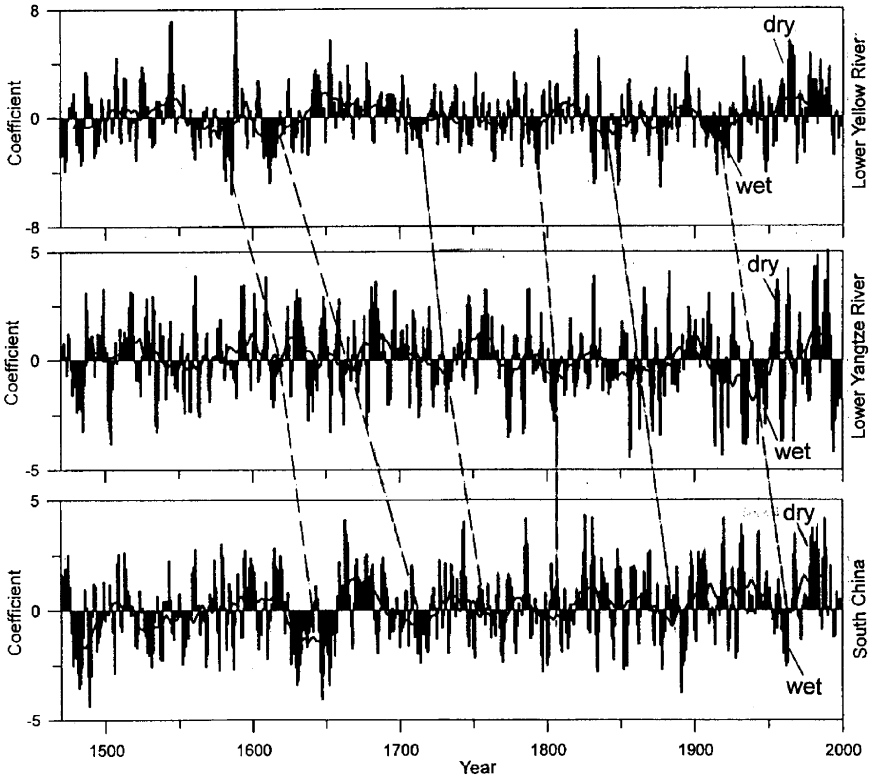

Fig. 5 Time series of three modes along (*upper*) the lower Yellow River (*B*), (*middle*) the lower Yangtze River (*C*) and (*lower*) south China (*D*) in Fig. 4, calculated from REOF. The *heavy line* denotes the 19-year running mean and the *dashed lines* join the wet maximum across the different valleys. A positive coefficient denotes dry climate

century accompanied by significant warming in the region (Qian and Zhu 2001).

In the middle and lower Yangtze River, the occurrence frequency of severe dry-wet was low in the eighteenth century. In the nineteenth century there was a trend of increasing frequency. Recently in the 1970s, the frequency of severe dry conditions reached 19%. The frequency of severe wetness has exceeded 10% from the early twentieth century.

There was no obvious trend in the frequency of severe dry-wet periods in southwest China before the nineteenth century but a significant rising trend in both severe dryness and wetness can be noted in Fig. 6 since the beginning of the nineteenth century. Recently, the frequency of severe dryness has exceeded 10% since the 1970s. The persistent severe wet conditions in the early twentieth century covered 15% of the time. The situation in south China is similar to that in southwest China but the phases are delayed.

6 Variations in WI

Now, we extend the analysis to the last millennium using the WI data series. We first applied a 5-year running mean filter to the WI series from AD 952 to 1997 for the Yellow River valley, the Yangtze River valley, and south China. The results are shown in Fig. 7. Along the Yellow River, relatively wet periods (positive WI) continued from the late fourteenth to the early fifteenth century, and reappeared in the late seventeeth century, the middle eighteenth century, and from the late nineteenth to the early twentieth century. Relatively dry periods (negative WI) are found in the early thirteenth century, late fifteenth century, early seventeenth century, and the middle twentieth century. Along the Yangtze River, relatively high frequency appeared from the seventeenth century to the early twentieth century. In south China, the frequency of dry-wet alternation was higher than in the Yellow River, particularly from the ninth to the fourteenth century.

To examine the frequency variation of wet and dry periods in the last millennium, we applied wavelet transform methods to these series. The results for the three regions are shown in Fig. 8. The distributions of $W(a, b)$ in the three panels of Fig. 8 show significant variations with dominant modes with time scales from 20 to 70–80 years. Variations at similar time scales, 20, 35, and 70 years, also were reported in previous studies (Wang and Zhao 1979; Liu 1992; Yan 1999). By Inspecting the time-scale of 70 years (heavy solid line) in the three panels, we can easily finds that the phase in the Yellow River leads that in the Yangtze River and south China.

In the recent centuries, centennial scale variations of wetness had different characteristics in the three regions. In the Yellow River region, wetness prevailed in the late nineteenth-early twentieth century and near average conditions in 1950s–1960s. In the Yangtze River region, frequent severe wetness happened in the early twentieth century and in recent years. The most recent wet period associated with the centennial variation in south China appeared in the mid twentieth century. From the later

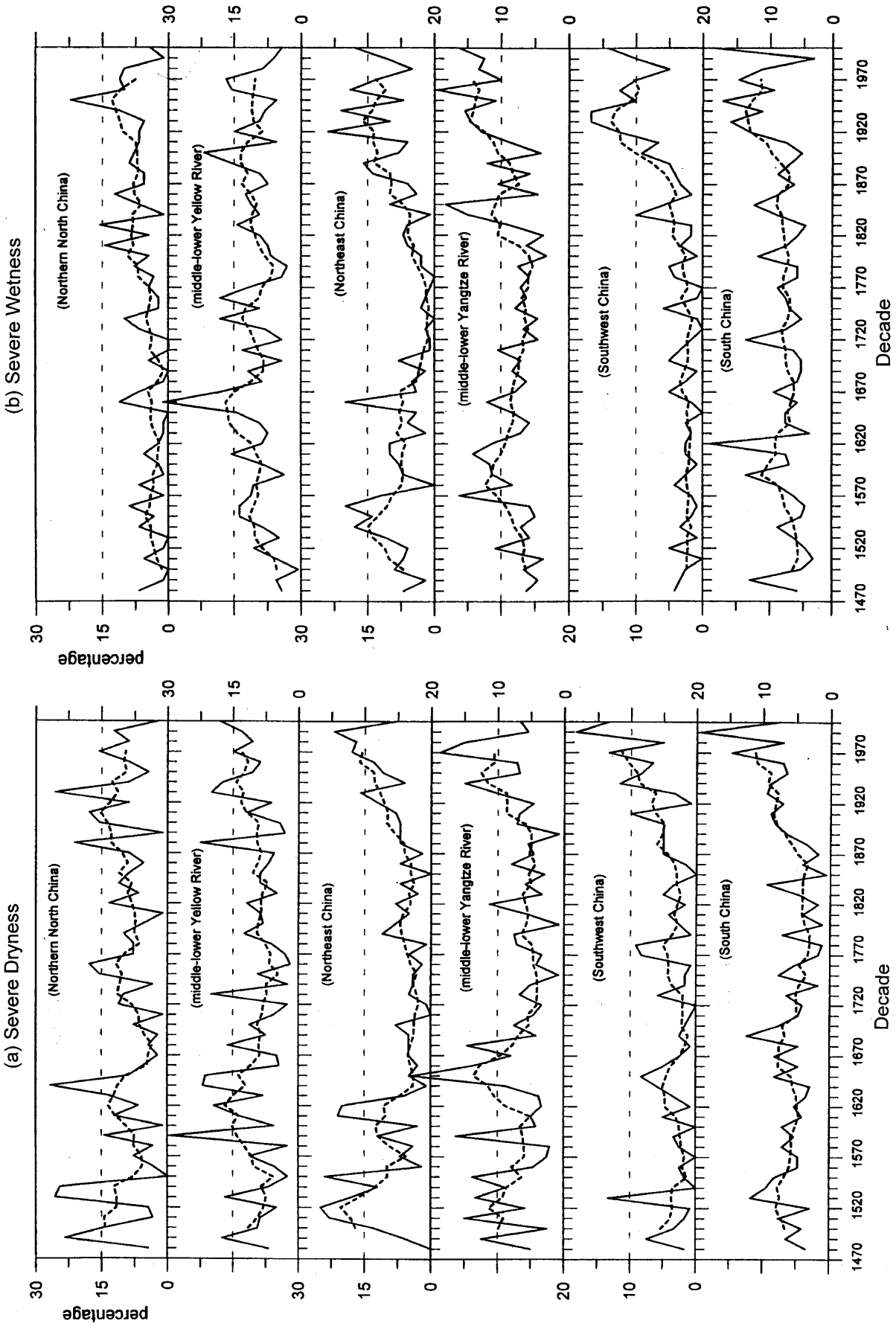

Fig. 6 Percentages of severe dryness and severe wetness in the six numerical regions in Fig. 1. *Dashed lines* indicate the five-point running mean

sixteenth century to the twentieth century, the 6–7 dry-wet spells in Fig. 8 are compared to those shown in Fig. 5 from the DWI data However there are unmatched start and end times due in part to different resolutions and coverage of the two data series.

7 Centennial-scale changes

In East Asia, the summer rainfall in eastern China, the Korean Peninsula, and Japan, often results from a circulation regime referred to as the summer monsoon front, which also is referred to as the *Meiyu* in China, the *Changma* in Korea, and the *Baiu* in Japan (Qian et al. 2002). Figure 3 shows the mean and standard deviation of the summer rainfall only in mainland China based on the stational data in the second half of the twentieth century. One of the rainfall centres with a large standard deviation is located in the lower Yangtze River. To reveal a compete picture in the centennial-scale variations of climate in East Asia, we need to analyze long-term series from these three different countries.

In this section, we first present analysis results using the South Korea precipitation dataset (1777–1997), which is one of the longest quantitative precipitation descriptions in the world. In this dataset, Jung et al. (2000) identified two centennial scale wet periods: 1783–1883 and 1911–1996. To extract the information for various other time scales, we applied wavelet transform to the annual precipitation data. Figure 9a shows the wavelet coefficients for the time scales 30–120 years over the period from 1777 to 1997. It is clear that at the 120-year time scale the wet periods occurred in 1808–1867 and in recent decades since 1930. The interdecadal oscillations appeared mainly at the 60–70 year time scale and the 30–40 year time scale. At the 60–70 year time scale, the dry peaks were near years 1840, 1898, and 1958. A recent wet peak developed around 1990. These dry and wet alternations were similar to that which appeared south of the Yangtze River (Qian and Zhu 2001). However, the variations in the South Korean annual precipitation series shows that the dryness was much severe, particularly between 1890–1910 and near 1777. The dry-wet transition in the last century occurred around 1915.

These variations in South Korea were quite different from those in eastern China. Figure 9b and c shows the wavelet transform of the wetness indices based on the ZI in regions A and D along the east coasts of China (Fig. 1). In region A, the wettest period appeared in 1877–1897, opposite to that of the precipitation anomalies in South Korea. In the recent two decades, dry climate was dominant in region A but more precipitation fell in South Korea. In the meantime, the sign of rainfall anomaly in region A is opposite to that in region D. This indicates that if a dry climate period occurs in north China, wet weather appears to the south of the Yangtze River and in South Korea. A transition of the dry-wet situation can be seen in the year 1977 at the 70-year time scale. Before that year, the wet climate occurred in north China with dryness in the south of the Yangtze River and South Korea. Since the late 1970s, wet weather has persisted south of the Yangtze River and in South Korea while dryness prevailed in north China.

The strong signal at the 60–70 year time scale also appears in regions B and C along the east coast of China

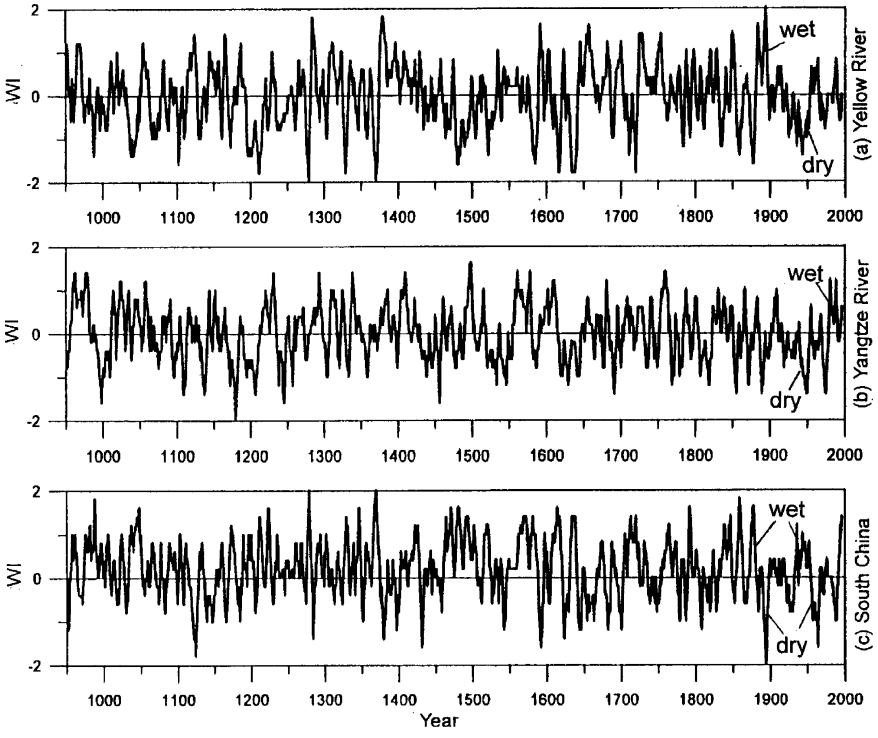

Fig. 7 WI series after 5-point running mean for the Yellow River, the Yangtze River, and south China from 952 to 1997. Positive values denote wet climate

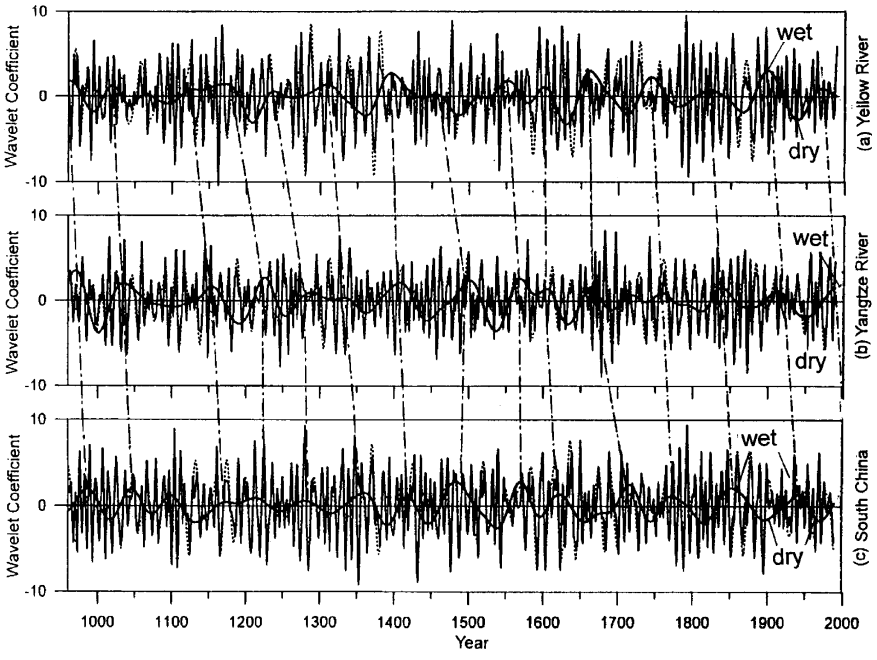

Fig. 8 Wavelet transform coefficients of WI series in **a** the Yellow River valley, **b** the Yangtze River valley, and **c** south China with 20-year, 35-year (*dotted line*) and 70-year time scales. The *dashed lines* connect the wet maximum across the different valleys. Positive coefficients denote wet climate

(Fig. 1). The same dry-wet alternations developed concurrently in regions A and B or in the regions C and D and in South Korea. In total rainfall anomalies in northern China (regions A and B) are opposite to those in southern China (region D) and South Korea.

8 Monsoon circulation changes

Rainfall in East Asia is directly connected with the southwesterly flow associated with the summer monsoon in the region. In China, summer rainfall changes in four "phases" (Nitta and Hu 1996; Liang and Wang 1998; Qian et al. 2002). The first phase starts in May and is called "pre-rainy season" in south China. In the second phase from mid June to mid July, the major rain belt moves northward to the lower Yangtze River Basin. In the third phase from late July through August, the rain belt migrates further north and major rainfall occurs in north China. In the fourth phase during September, the rain belt quickly retreats southward and rain returns to southeast China. These rainfall phases are consistent with the northward expansion of 850 hPa southwesterly winds in East Asia (Qian et al. 2002). Resulting from this information, we have chosen the three months (June–August) circulation to investigate dry-wet anomalies in the lower Yellow River and the lower Yangtze River basins.

Figure 10 shows the 850 hPa summer winds averaged from 1954 to 1976 (a wet period in north China) and from 1977 to 1999 (a dry period in north China), using the Reanalysis data. In the two periods, different patterns of summer monsoon circulation can be found over East Asia, particularly from eastern China to the Korean peninsula. In the summers of 1954–76 (Fig. 10a), strong southerly-southwesterly winds reached north and northeast China. The summer monsoon was strong and rainfall concentrated in northern China (regions A and B). Also, a stronger than average subtropical high influenced southern China and South Korea (marked by E), creating a dry climate in region D (lower Yangtze River) and South Korea. However, in the summers of 1977–99 (Fig. 10b), very weak southerly winds were found in East Asia. The southwesterly winds only reached the south of the lower Yangtze River (region D) and South Korea. This pattern may explain why the summer floods frequently occurred in southern China and South Korea in the recent two decades.

Since the mid 1970s, the tropical sea surface temperature (SST) also has experienced a transition (Wang 1995; Qian et al. 1999). Previous studies show that there are some linkages or influences between SST and the monsoon rainfall in Asia (Yang and Lau 1998; Weng et al. 1999). To explain the change of East Asian summer monsoon circulations in recent decades, we show in Fig. 11 the summer season 1000 hPa temperature difference between 1977–99 and 1954–76, again using the Reanalysis data. In Fig. 11, a cooling of the summer surface air temperature is observed in the Asian inland regions and a warming of the temperature over the oceans. Therefore, the thermal contrast between the continent and the surrounding ocean has been reduced in the recent two decades. This weakened thermal contrast may explain the weak summer monsoon circulation in the recent two decades.

Global warming is remarkable in the last century but regional differences in temperature changes have also been experienced in many places over the world. From Fig. 11 the significant warming can be noted in the mid- and high latitudes while cooling is shown in Asian inland regions during the last two decades. In the North Pacific

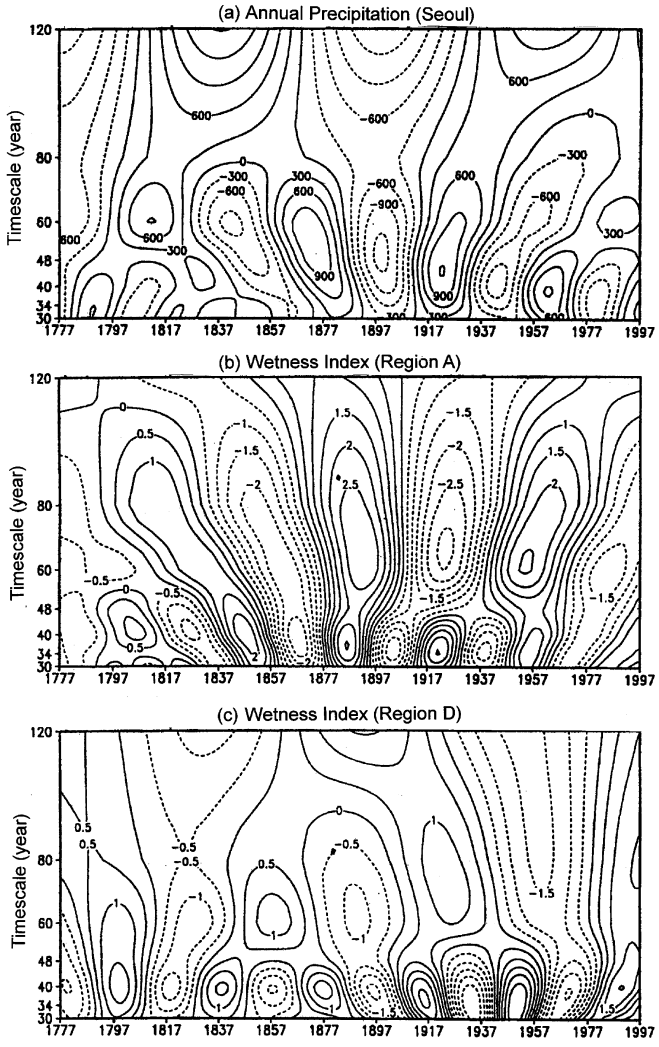

Fig. 9 The coefficients of wavelet transform of the precipitation series from Seoul, Korea, and wavelet transform of the ZI series for region A, and region D, from 1777 to 1997. The *dashed lines* denote dry periods

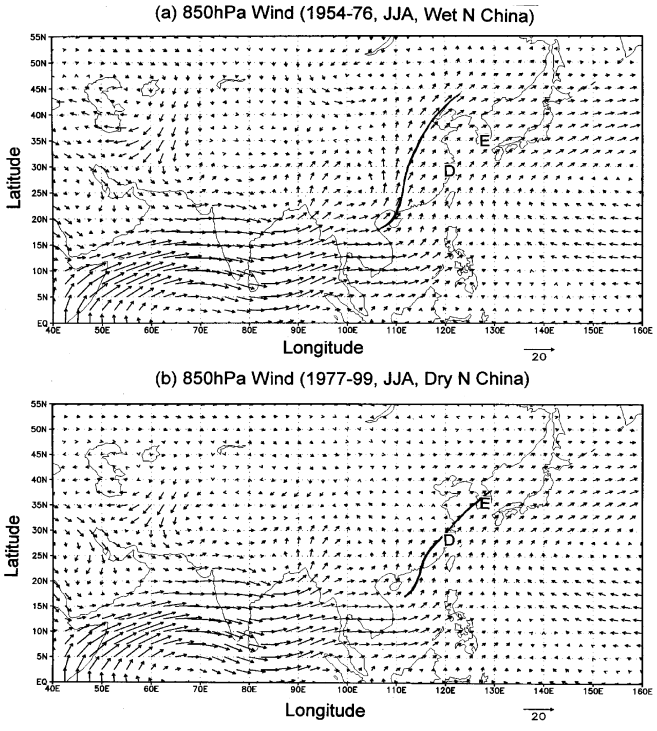

Fig. 10 Mean summer (June–July–August) 850 hPa winds (ms^{-1}) averaged **a** from 1954 to 1976 and **b** from 1977 to 1999. The *heavy-solid lines* denote the southwesterly flows in East Asia. Letters *D* and *E* indicate the positions of the lower Yangtze River and South Korea

basin, changes in SST have been noted with warming in the low latitudes and cooling in the northwest North Pacific since the mid 1970s (Wang 1995; Qian et al. 1999). The air temperature (Fig. 11) also shows a response to the changes in the SST. By applying wavelet transform to the last 500-year El Niño-La Nino indices, Zhu et al. (1999) found six persistent patterns of the indices and their variations since the 1550s that were connected with variations in the Indian monsoon rainfall. El Niño-La Nina indices are defined as five numerical values representing different El Niño and La Nina intensities, with 2 for very strong El Niño, 1 for strong El Niño, 0 for normal, –1 for strong La Nina, and –2 for very strong La Nina years. We focus on the recent persistent patterns, one with more El Niño events (warmer tropics) in 1900–1930 and 1970–2000, and the other with more La Nina events (cooler tropics) in 1940–1960. We found that the warmest period in northwest China appeared in the 1940s for the surface air temperature (Qian and Zhu 2001). Thus, the strengthened thermal contrast between the tropical ocean and the Asian inland region in the period 1940–1960 led the strong East Asian monsoon and more rainfall in north China. The weakened thermal contrast during the two periods 1900–1930 and 1970–2000 was associated with weaker monsoon and below normal rainfall in north China (Fig. 9).

9 Concluding remarks

Annual series of dry-wet intensity for the last one thousand years, based on historical documents and recent observations, have been used to investigate the climate variations in East Asia. Major results show a 70-year alternation of the dry-wet conditions in different regions in East Asia and migration of the wet-dry anomalies from northern to southern China (including South Korea). The results were further confirmed by the time series of different modes and dry-wet indices in the lower Yellow River, the lower Yangtze River, south China, and South Korea, as well as observation records from other independent sources.

Dryness and wetness data set for the 530 years (1470–1999) derived from Chinese historical documents and summer season rainfall at 100 sites in eastern China were used to examine trends in the occurrence frequency of

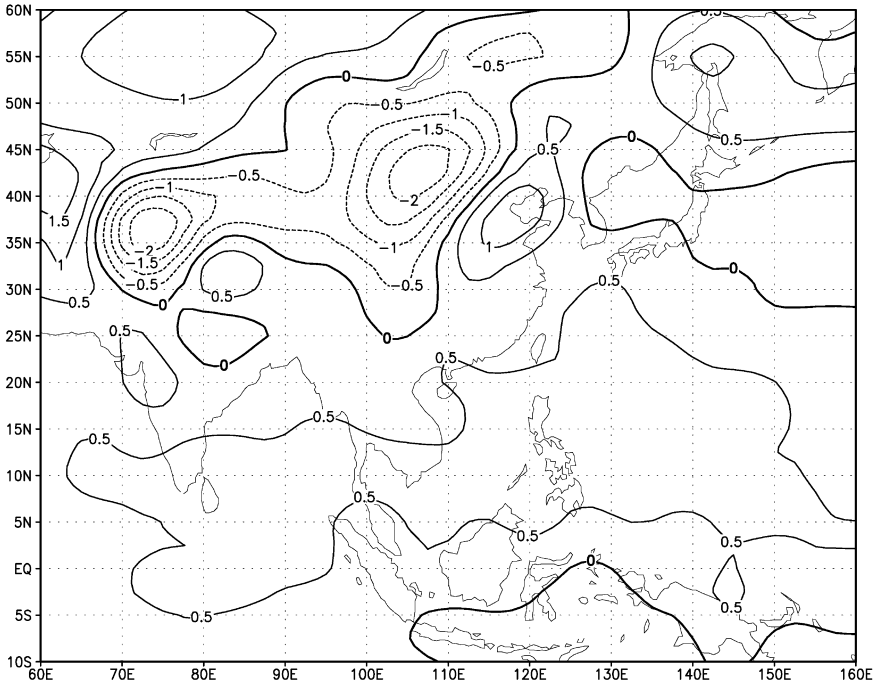

Fig. 11 Variations in the 1000 hPa summer surface air temperature (°C) between 1977–1999 and 1954–1976

extreme dryness and wetness. Our analysis indicates that frequency of severe dryness and severe wetness increased in eastern China since the early twentieth century. Apparently this trend has appeared along with the recent global warming (Jones 1994; Fu et al. 1999) and the regional climatic changes in China (Qian and Zhu 2001). The trend may partially explain the enhanced interannual variability in dryness and wetness in the recent decades in China as elaborated in Yan (1994).

We have shown that our indices DWI, WI, and ZI can reasonably reveal the dry-wet oscillations and the oscillation phase in East Asia. Detailed comparisons of these oscillations in China are made with observed rainfall variations in Seoul, Korea, for the period 1777–1999. Results show fairly consistent variations at centennial scales, indicating that China and South Korea are strongly influenced by the East Asian monsoon systems. Severe dryness and severe wetness in the region are direct responses to the East Asian monsoon strength variation. In the past 50 years, phases with the relatively strong monsoon were found in the 1960s and a weaker monsoon since the 1980s. In the period of strong monsoons, there was more precipitation in northern China and a dry climate in southern China and South Korea.

The surface air temperature difference between the two periods 1954–76 and 1977–99 shows that the summer temperature in inland Asia has become cooler and the temperature over the oceans surrounding the continent has become warmer. These changes have resulted in weakening in the thermal contrast between the continent and its surrounding oceans. This weakened thermal contrast may further have been attributed to the weaker summer monsoons in the recent two decades.

Acknowledgements We wish to thank the two anonymous reviewers and the editor, Dr. Elisa Manzini, whose comments and suggestions helped improve the clarity of this work. This study is jointly supported by the doctorial project of the Ministry of Education of China (20010001052), the National Key Program for Developing Basic Sciences in China (G1999043405), and the project of the Chinese Academy of Science (ZKCX2-SW-210).

References

Bradley RS, Jones PD (1992) Climate since AD 1500. In: Bradley RS, Jones PD (eds) Climate since AD 1500 Routledge, London, pp 1–16

Brunet Y, Collinean S (1994) Wavelet analysis of diurnal and nocturnal turbulence above a maize crop. In: Foufoula-Georgiou E, Kumar P (eds) Wavelets in geophysics Academic, San Diego, USA, pp 129–150

Central Meteorological Bureau (1981) Atlas of flood and drought in China in the last 500 years. Cartological Press, Beijing, China, p 332

Cho H-K, Na I-S (1979) Changes in climate in Korea during the eighteenth century-centering on rainfall amount (in Korean). J Korean Studies 22: 83–103

Damage Report (1995) Report of the damage caused by disaster in China. China Statistical Press, Beijing, China, pp 406

Fu C-B, Diaz HF, Dong D-F, Fletcher JO (1999) Changes in atmospheric circulation over Northern Hemisphere oceans associated with the rapid warming of the 1920s. Int J Climatol 19: 581–606

Hu Q, Feng S (2001) A southward migration of centennial-scale variations of drought/flood in eastern China and the western United States. J Clim 15: 1323–1328

Jiang J-M, Zhang'D, Fraedrich K (1997) Historical climate variability of wetness in East China (1960–1992): a wavelet analysis. Int J Climatol 17: 968–981

Jones PD (1994) Recent warming in global temperature series. Geophys Res Lett 21: 1149–1152

Jung H-S, Lim G-H, Oh J-H (2000) Characteristics of the instrumental precipitation records during the last 220 years in Seoul, Korea. Proc climate change and variability and the 29th international geophysical congress, August 9–13, 2000, Konkuk University, Seoul, S. Korea

Kalnay E, Kanamitsu M, Kister R, Collins W, Deaven D, Gandin L, Iredell M, Saha S, White G, Wollen J, Zhu Y, Chelliah M, Ebisuzaki W, Higgins W, Janowiak J, Mo KC, Ropelewski C, Wang J, Leetmaa A, Reynolds R, Jenne Roy, Joseph Dennis (1996) The NCEP/NCAR 40-year Reanalysis Project. Bull Am Meteorol Soc 77: 437–471

Kelly PM, Jones PD (1999) Spatial patterns of variability in the global surface air temperature data set. J Geophys Res 104: 24,237–24,256

Kim YO (1992) The Little Ice Age in Korea: an approach to historical climatology. In: Mikami T (ed) Proc Int Symp on the Little Ice Age Climate, Department of Geography, Tokyo Metropolitan University, pp 170–175

Kim B-J, Kripalani RH, Oh J-H, Moon S-E (2002) Summer monsoon rainfall patterns over South Korea and associated circulation features. Theor Appl Climatol 72: 65–74

Kistler R, et al (2001) The NCEP-NCAR 50-year reanalysis: monthly means CD-ROM and documentation. Bull Am Meteorol Soc 82: 247–267

Lau K-M, Weng H-Y (1995) Climate signal detection using wavelet transform: how to make a time series sing. Bull Am Meteorol Soc 76: 2391–2402

Liang XZ, Wang WC (1998) Association between China monsoon rainfall and tropical jets. QJR Meteorol Soc 124: 2597–2623

Lim G-H, Jung H-S (1992) Interannual variation of the annual precipitations at Seoul, 1771–1990. J Korean Meteorol Soc 28: 125–132

Lim G-H, Jhun J-G (1996) Assessment of climatological precipitation amount in the Korean Peninsula in terms of the precipitation records of Korea Raingauge and precipitation model output (in Korean). Rep KOSEF 93-0700-06-02-3, Department of Atmospheric Sciences, Seoul National University, pp 165

Liu W-L (1992) Changes of drought and flood during the latest 230 years in the Yellow River basin. In: Mikami T (ed) Proc Int Symp Little Ice Age Climate, Department of Geography, Tokyo Metropolitan University, Japan, pp 308–314

Lu R-Y (2001) Interannual variability of the summertime north Pacific subtropical high and its relation to atmospheric convection over the warm pool. J Meteorol Japan 79: 771–783

Murata A (1992) Reconstruction of rainfall variation of the Baiu in historical times. In: Bradley RS, Jones PD (eds) Climate Since AD 1500. Routledge, London, pp 224–245

Nitta Y, Hu ZZ (1996) Summer climate variability in China and its association with 500 hPa height and tropical convection. J Meteorol Soc Japan 74: 425–445

Qian W-H, Kang H-S, Lee D-K (2002) Distribution of seasonal rainfall in the East Asian monsoon region. Theor Appl Climatol 73: 151–168

Qian W-H, Zhu Y-F (2001) Climate change in China from 1880 to 1998 and its impact on the environmental condition. Clim Change 50: 419–444

Qian W-H, Zhu Y-F, Ye Q (1999) Interannual and interdecadal variabilities in SST anomaly over the eastern equatorial Pacific. Chin Sci Bull 44: 568–571

Qian W-H, Zhu Y-F (2002) Little Ice Age climate near Beijing, China, inferred from historical and stalagmite records. Quat Res 57: 109–119

Richman MB (1981) Obliquely rotated principal components: an improved meteorological map typing technique? J Appl Meteorol 14: 1223–1235

Richman MB (1986) Review article, rotation of principal components. J Clim 6: 293–35

Ronberg B, Wang WC (1987) Climate patterns derived from Chinese proxy precipitation records: an evaluation of the station networks and statistical techniques. J Climatol 7: 391–416

Song J (1998) Reconstruction of the southern oscillation from dryness/wetness in China for the last 500 years. Int J Climatol 18: 1345–1355

Song J (2000) Changes in dryness/wetness in China during the last 529 years. Int J Climatol 20: 1003–1015

Tang Z (1988) The reconstruction of climate in historical times for small area. In: Zhang J (ed) The reconstruction of climate in China for historical times. Science Press, Beijing, China, pp 10–17

Wang B (1995) Interdecadal changes in El Niño onset in the last four decades. J Clim 8: 267–285

Wang S-W (1988) Wetness variation in China over the last 500 years. In: Zhang J (ed) The reconstruction of climate in China for historical times. Science Press, Beijing China, pp 66–78

Wang S-W, Zhao Z-C (1979) The 36-year wetness oscillation in China and its mechanism (Chinese with English abstract). Acta Meteorol Sinica 37: 64–73

Wang S-W, Zhao Z-C, Chen Z-H, Tang Z-G (1987) Drought/flood variations for the last two thousand years in China and comparison with global climatic change. In: Ye DZ, Fu CB, Chao JP, Yoshino M (eds) The climate of China and global climate. China Ocean Press, Springer Berlin Heidelberg New York, pp 20–29

Weng H-Y, Lau K-M, Xue Y-K (1999) Multi-scale summer rainfall variability over China and its long-term link to global sea surface temperature variability. J Meteorol Soc Japan 77: 845–857

Yan ZW (1994) Evolutions of the spectra of historical flood drought fluctuations. Chinese Sci Bull 39: 664–669

Yan ZW (1999) Interdecadal oscillations of precipitation in North China and its relation with global temperature change (Chinese with English abstract). Q J Appl Meterol 10: 16–22

Yan ZW, Yang C (2001) Influence of inhomogeneity on the estimation of mean and extreme temperature trends in Beijing and Shanghai. Adv Atmos Sci 18: 309–322

Yan ZW, Jones PD, Davies TD, Moberg A, Bergstrom H, Camuffo D, Cocheo C, Maugeri M, Demaree GR, Verhoeve T, Thoen E, Barriendos M, Rodriguez R, Martin-Vide J, Yang C (2002) Trend of extreme temperatures in Europe and China based on daily observations. Clim Change 53: 355–392

Yang S, Lau KM (1998) Influence of sea surface temperature and ground wetness on Asian summer monsoon. J Clim 11: 3230–3246

Yao CS (1982) A statistical approach to historical records of flood drought. J Appl Meteorol 21: 588–594

Zhang'D (1988) The method for reconstruction of the dryness/wetness series in China for the last 500 years and its reliability. In: Zhang J (ed) The reconstruction of climate in China for historical times. Science Press, Beijing, China, pp 18–30

Zhao ZG, Wang YG et al. (eds) (1999) Summer drought/flood in China and circulation fields. China Meteorological Press, Beijing, China, p 297

Zhang J, Crowley TJ (1989) Historical climate records in China and reconstruction of past climates. J Clim 2: 833–849

Zhou YK, Ma ZY, Wang LH (2002) Chaotic dynamics of the flood series in the Huaihe river Basin for the last 500 years. J Hydrol 258: 100–110

Zhu YF, Qian WH, Ye Q (1999) Tropical sea surface temperature anomaly and Indian summer monsoon. Acta Meteorol Sinica 13: 154–163

Zhu JH, Wang SW (2001) 80a-oscillation of summer rainfall over the east part of China and east-Asian summer monsoon. Adv Atmos Sci 18(5): 1043–1051